Journal of Alloys and Compounds 509 (2011) 7784–7788

Contents lists available at ScienceDirect

Journal of Alloys and Compounds

journal homepage: www.elsevier.com/locate/jallcom

Metal transition doping effect on the structural and physical properties of delafossite-type oxide $CuCrO_2$

F. Jlaiel [a], M. Amami [a,b,*], N. Boudjada [b], P. Strobel [b], A. Ben Salah [a]

[a] Laboratoire des Sciences de Matériaux et d'environnement, Faculté des Sciences de Sfax, BP 763, 3038 Sfax, Tunisia
[b] Institut Néel, CNRS et Université Joseph Fourier, B.P. 166, 38042 Grenoble Cedex 9, France

ARTICLE INFO

Article history:
Received 2 December 2010
Received in revised form 27 April 2011
Accepted 28 April 2011
Available online 8 May 2011

Keywords:
Delafossite
Non magnetic impurity
XRD
Magnetic susceptibility
Raman spectroscopy

ABSTRACT

In this paper we reported on the non magnetic substitution effects on the structural, spectroscopic, and magnetic properties of the $CuCrO_2$ delafossite. The incorporation of M^{3+} generates very anisotropic microstrains in the structure beside a magnetic dilution. The temperature dependence of all samples exhibits paramagnetic behavior at high temperature. It is argued that non magnetic-substitution destabilizes the antiferromagnetic order of Cr^{3+} ions and modulates the spin configuration leading to a weak ferromagnetism. The coupling between the magnetic order and ferroelectric order is also characterized.

1. Introduction

The delafossite oxide $CuMO_2$ (M = trivalent cation) is one of the number of systems possessing an antiferromagnetic triangular sublattice. $CuMO_2$ has a layered structure with a space group of $R\bar{3}m$, which is viewed as the alternate stacking of edge-shared MO_6 octahedral (MO_2) layers and Cu layers [1]. The magnetic properties of these layered compounds have attracted much attention, since the geometrical frustration in the magnetic triangular sublattice at the M sites causes intriguing properties, such as field induced multistep magnetization change [2] and multiferroics [3].

The possibility of mixing trivalent cations M and M′ on the M site in the delafossite structure may allow a compromise between desirable properties of each of AMO_2 and $AM'O_2$ if a solid solution can be achieved [4].

Recently, the effect of a small amount of substitution on magnetic ordering in a frustrated triangular lattice antiferromagnet $CuFeO_2$ has been studied by neutron diffraction, magnetic susceptibility and specific heat measurements on $CuFe_{1-x}Al_xO_2$ single-crystals with $x = 0.02$ and $x = 0.05$ [5]. With only a small amount of substitution, $x = 0.02$, the zero-field successive magnetic phase transitions with quasi-Ising character observed for $x = 0.00$ are entirely changed to successive phase transitions from a paramagnetic state to an incommensurate complex state through an incommensurate magnetic state, suggesting that the original Heisenberg spin character hidden in $CuFeO_2$ is retrieved.

$CuMO_2$ with M = Cr has also been studied for its thermodynamic [6], magnetic [7], optoelectronic [8–12], and thermoelectric [13,14] properties, catalytic activity [15], and lithium insertion [16]. $CuCrO_2$ delafossite is also a p-type semiconductor but with a lower intrinsic electrical conductivity ($\sigma_{RT} = 3.5 \times 10^{-5}$ S/cm) [9] because of difficulties in inducing an oxygen nonstoichiometric phase in this system. However, $CuCrO_2$ is a more promising TCO than $CuFeO_2$ because of good optical transparency in the visible range with a band gap of about 3.1 eV and with an electrical conductivity that can be drastically improved up to $\sigma_{RT} = 220$ S/cm with appropriate doping like in a $CuCr_{0.95}Mg_{0.05}O_2$ thin film [17,18]. We report on the substitution effects of non magnetic ions on the structure and magnetic properties of $CuCrO_2$.

2. Experimental

Polycrystalline $CuCr_{0.95}M_{0.05}O_2$ (M = Al, Co, Rh, and Sc) samples were synthesized by a standard solid-state reaction procedure. Starting reagents (Cu_2O, Cr_2O_3, CoO, Sc_2O_3, Rh_2O_3 and Al_2O_3 > 99.9%,) were weighted, mixed, and ground together, then calcined in air at 1000 °C for 12 h in an alumina crucible. The obtained mixture was ground again and calcined several times in air at 1050 °C for about 36 h with intermediate grinding. Samples were characterized by powder X-ray diffraction (XRD) measurements. The lattice parameters were obtained by Le Bail refinement. Raman spectroscopy measurement was conducted on a laser Raman spectrometer (Spectra Physics krypton ion laser) Magnetization dependence on temperature was measured in a quantum Design superconducting quantum interference device

* Corresponding author at: Institut Préparatoire aux études d'ingénieur de Nabeul, Compus universitaire Mrazka 8050 Nabeul, Tunisia. Tel.: +216 98 95 2547; fax: +216 72 22 0181.
E-mail address: mongi.amami@ipein.rnu.tn (M. Amami).

0925-8388/$ – see front matter © 2011 Elsevier B.V. All rights reserved.
doi:10.1016/j.jallcom.2011.04.153

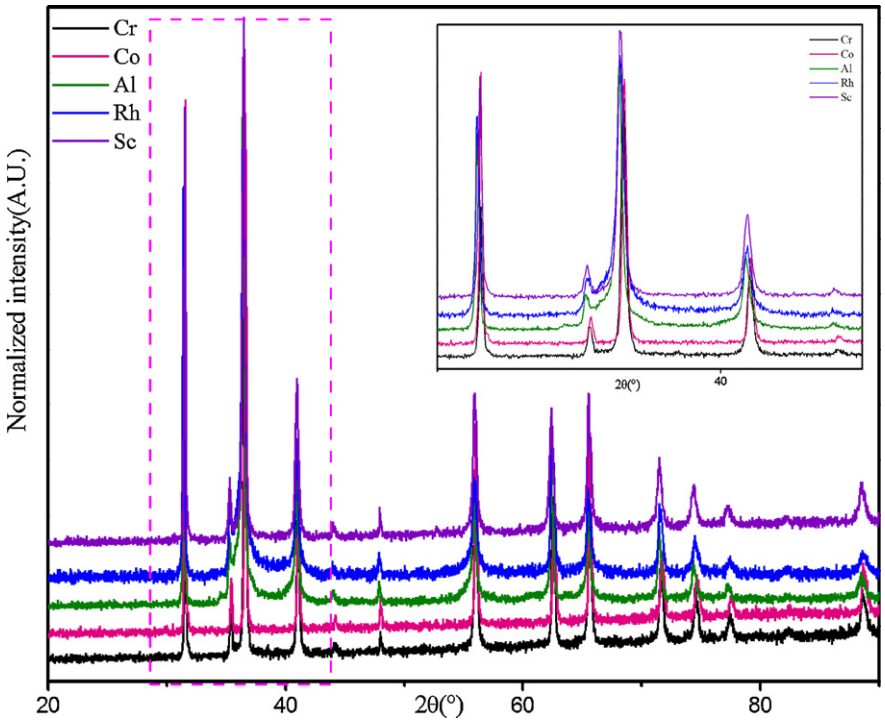

Fig. 1. XRD patterns of $CuCr_{1-x}M_xO_2$ samples for different M cations.

(SQUID) magnetometer while warming from 2 to 300 K in 0.1 T (zero field cooling ZFC).

3. Result and discussion

3.1. Structural properties

Fig. 1 shows the XRD patterns of $CuCr_{0.95}M_{0.05}O_2$ samples at room temperature. All reflections can be assigned to the single delafossite rhombohedral structure with space group $R-3m$ and no detectable impurity phase is observed. The lattice parameters a and c of the $CuCr_{1-x}M_xO_2$ (M = Al, Sc, Rh, Co and $x = 0.05$) samples with their corresponding errors are shown in Table 1. Since M^{3+} and Cr^{3+} have the same oxidation state, M^{3+} substitution for Cr^{3+} is expected to introduce mainly atomic disorder in the Cr network. In addition, Fig. 1 clearly shows that the Bragg peaks become broader for Al^{3+} and Rh^{3+} doped samples. This is probably related to the introductions of strains in the lattice, since Al^{3+} is a much smaller cation than Cr^{3+} [19]. These results are in good agreement with those reported by Okuda et al. [20].

However, for the Sc and Rh-doped samples, the change is rather anisotropic as it is mainly due to the shrinking of the a parameter whereas the c parameter remains more or less constant. As the Cu–O distance does not vary much in delafossite, this tendency reflects a flattening of the MO_6 octahedra. A nice geometric account of this evolution is given in [21] where the authors suggest that the strong repulsion between M^{3+} ions across the octahedron shared edges reduces the O–O distance to the contact distance. Therefore the increase of the size of M cation leads to an increase of the octahedron distortion and in turn of the M–M distance that corresponds to the a parameter. We may recall that in $CuMO_2$, as M changes from Al^{3+} to La^{3+}, the a parameter undergoes a huge increase from 2.8 up to 3.8 Å. This general trend is also observed at a smaller scale in the investigated samples.

Moreover, there is almostly, no measurable peak shift for samples due to the Co doping, indicating essentially the same lattice parameters for the samples. It can be concluded that the valence of Co ions was not Co^{2+} (HS) or Co^{3+} (L.S) according to the data of the ionic radius of Co and Cr (Co^{2+}(HS): 0.745 Å, Co^{3+}(HS): 0.61 Å, Co^{3+}(LS): 0.545 Å and Cr^{3+}: 0.63 Å) [19] as well as lattice expansion. The lattice parameters a and c would increase if the valence state of the Co ions is 2+(HS) in Co-doped $CuCrO_2$ semiconductors because the ionic radii of Co^{2+} are larger than that of Cr^{3+}. However it would decrease if the Co ions is 3+(LS). It can be confirmed that the valence state of Co ions is either 3+(HS) or 2+(LS). Moreover the changes in the lattice parameters a and c due Co-dopping are very small. Therefore, the valence state of the Co ions presented in the samples should be 3+ since the ionic radius of Co^{3+}(HS) is slightly smaller than that of Cr^{3+}, whereas the valence state of Co ions cannot be totally confirmed by the changes in the lattice parameters.

3.2. Raman spectroscopy

The delafossite structure belongs to point group C3v and space group $R-3m$. The four atoms in the primitive cell of its rhombohedral $R-3m$ structure give rise to 12 optical phonon modes ($\Gamma = A_{1g} + E_g + 3A_{2u} + 3E_u$) in the zone center ($k \sim 0$): three acoustic and nine optical modes. Among these, the two phonons modes with A_{1g} and E_g symmetry are Raman-active. The former

Table 1
$CuCrO_2$ cell parameter evolution the with chemical impurities.

	Cr	Al	Co	Rh	Sc
a (Å)	2.9775(1)	2.97318(2)	2.9743(3)	2.9787(5)	2.9831(1)
c (Å)	17.1169(1)	17.0922(3)	17.1133(2)	17.109(3)	17.1125(3)

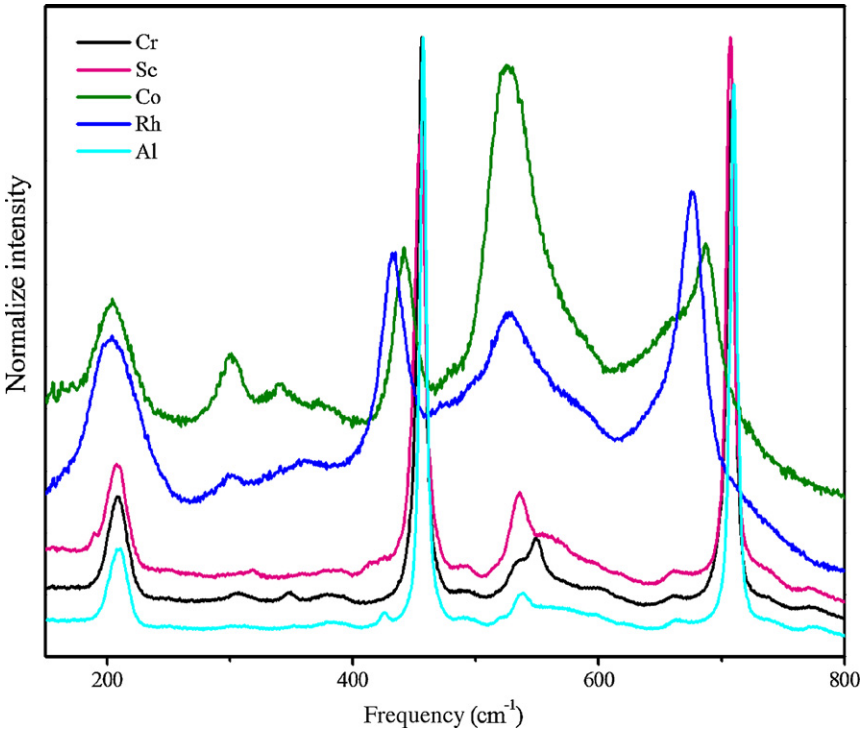

Fig. 2. Room temperature Raman spectra of 5% doped $CuCrO_2$.

assigned to the Cu–O bond vibration along the *c*-axis, whereas the doubly degenerate E-modes describe the vibration along the *a*-axis.

Fig. 2 shows the Raman spectra of $CuCr_{1-x}M_xO_2$ for different doped samples using a 514.5 nm laser wavelength excitation. The Raman spectrum of $CuCrO_2$ shows three typical vibrational bands of delafossite structure, in agreement with earlier results on $CuAlO_2$ [22] and $CuGaO_2$ [23]. These bands are identified as $\sigma(A_{1g})$ at 691 cm^{-1}, $\sigma(E_g)$ at 444 cm^{-1} and $\sigma(A_g)$ at 207 cm^{-1} (see Fig. 2). It has been suggested that these vibrations may be associated with the spectral features of edge-sharing $Cr^{III}O_6$ octahedra and possibly the O–Cu^{I}–O linear bond [24]. As shown in Fig. 2, M^{3+} substitution induces abrupt changes in frequency and in linewidth of the A_{1g} and E_g modes. The frequencies shift to shorter wavenumbers, indicating a weakening of (Cr,M)–O bonding, and is consistent with the observed lattice expansion along the different axes and the difference in ionic radius between Cr^{3+} and M^{3+}. The A_{1g} mode, in particular, is shifted by up 35 cm^{-1} upon Rh substitution; its frequency is thus very sensitive to M-site atom-oxygen bonding characteristics. For Co and Rh-doped samples, we also note a strong increase in intensity of the initially weak band around 535 cm^{-1}, the A_{1g}–E_g mode magnitude ratio is reverted and shoulders appear on several bands. We suggest that these features are related to increased disorder. These results confirm that these substitutions are possible while maintaining the delafossite structure. However, local changes do arise, and they are much more relevant in Raman spectroscopy that is a local probe than in X-ray diffraction, where the effects of cationic composition changes are averaged and show up mainly as peak broadening.

3.3. Magnetic properties

Fig. 3 shows the temperature dependence of the magnetization (*M*–*T* curve) of the $CuCr_{1-x}M_xO_2$ (M = Al, Sc, Rh, Co and $x = 0.05$) samples, where a 0.1 T magnetic field was applied. The inset of Fig. 3 shows the region of the dotted line in Fig. 3 in order to clearly present the *M*–*T* curves at a low temperature. It can be clearly seen that all the samples are in a paramagnetic states above 150 K.

The magnetization of the samples changes with changing M element. For $x = 0.00$, an anomaly appears at 26 K owing to an antiferromagnetic (AFM) transition. The Néel temperature (T_N) is almost consistent with the one previously reported [25]. For Rh-doped sample the *M*–*T* curves exhibit similar shapes when the temperature is greater than 30 K. Abrupt increases in magnetization appear at about 100 K shown in Fig. 3. It implies a FM transition which should be due to the FM interaction through the Rh^{3+}–O–Cr^{3+} exchange.

Both Co doped and Al-doped samples exhibit a weak paramagnetism varying slightly with temperature. Such behavior is reported for Co^{+3} ions is low spin (LS) configuration. The value of magnetic susceptibility ($\chi_{300\,K} = 3.54 \times 10^{-3}$ uem Oe^{-1} mol^{-1} for instance for cobalt doped) is however much higher than expected for an oxide containing just copper (I) and Cr(III) and cobalt (III) (LS) cations. The origin of this behavior could result from small amounts of magnetic impurities such as Co^{2+}(HS) ions which could be due to slight departure from stoichiometric composition.

The magnetization reaches a maximum at 25 K and then decreases for cobalt doped sample, which is attributable to the AFM transition. The very slight distortion in Co-doped sample makes sure that spin–orbit coupling is not destroyed. Whereas the AFM transition does not appear in the whole temperature range for Sc- and Al-doped samples. But then a tiny anomaly in the *M*–*T* curves can be seen at about 30 K, which is due to the AFM interaction. These doping induced changes are qualitatively different from those for the Rh^{3+} and Co^{3+} doping and are expected when only randomness is introduced.

For Rh-doped sample, the FM transition temperature (Curie temperature T_C) is about 120 K. The FM interaction is clearly stronger than the AFM interaction as Rh doped Cr. All these changes in the *M*–*T* curves indicate a competition between AFM and FM interactions for Sc and Al-doped samples, and also indicate that the double exchange (DE) interaction between the Al^{3+}, Sc^{3+} and Cr^{3+} ions is weaker in these systems.

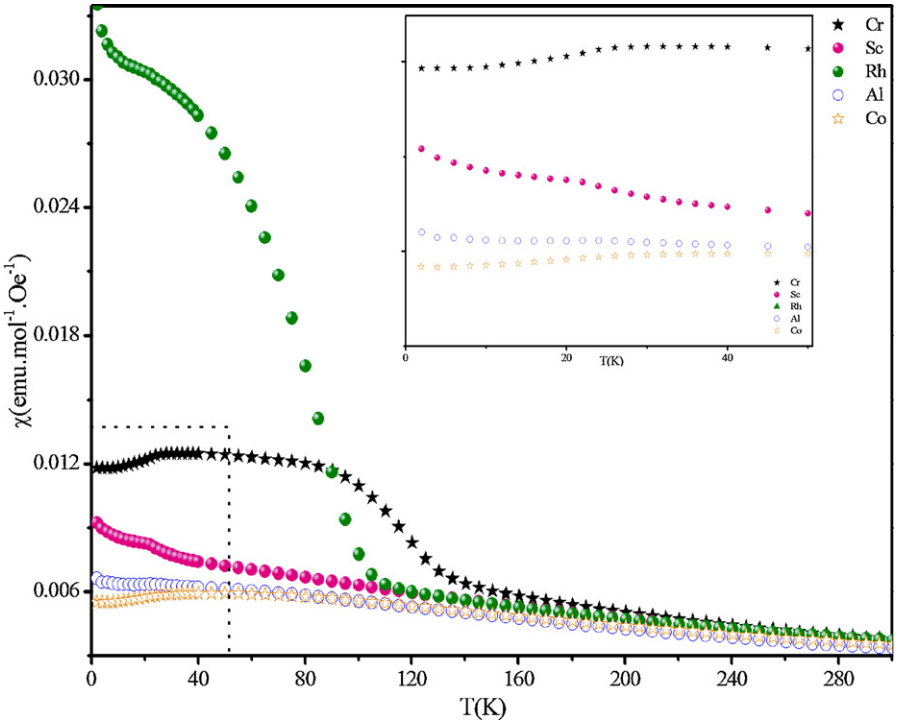

Fig. 3. Magnetic susceptibility evolution of $CuCrO_2$ with the chemical impurities.

One of the possible factors affecting the physical properties may be, in addition to the doped holes and magnetic randomness, a structural change in the lattice stemming from the substitution of the ions. The change in the lattice constants introduced by the Rh doping falls between the changes due to the Sc doping and the Al doping. The change in lattice constant does not directly induce the change in M, since the Rh-doped compound with the least change in lattice constant shows the largest change in M with the substitution.

Plots of the inverse molar susceptibility $1/\chi$ as a function of the temperature for the $CuCr_{1-x}M_xO_2$ (M = Al, Sc, Rh, Co and $x = 0.05$) samples are shown in Fig. 4. The plot of $1/\chi$ versus T shows an exactly linear relation at high temperature, which is well fitted by the Curie–Weiss equation, $\chi = C/(T + \Theta)$. Estimated values of C and Θ are given in Table 2. It indicates that all the doped samples are paramagnetic states at high temperature, while the curves show some nonlinear behavior attributed to AFM or FM interaction at low temperature.

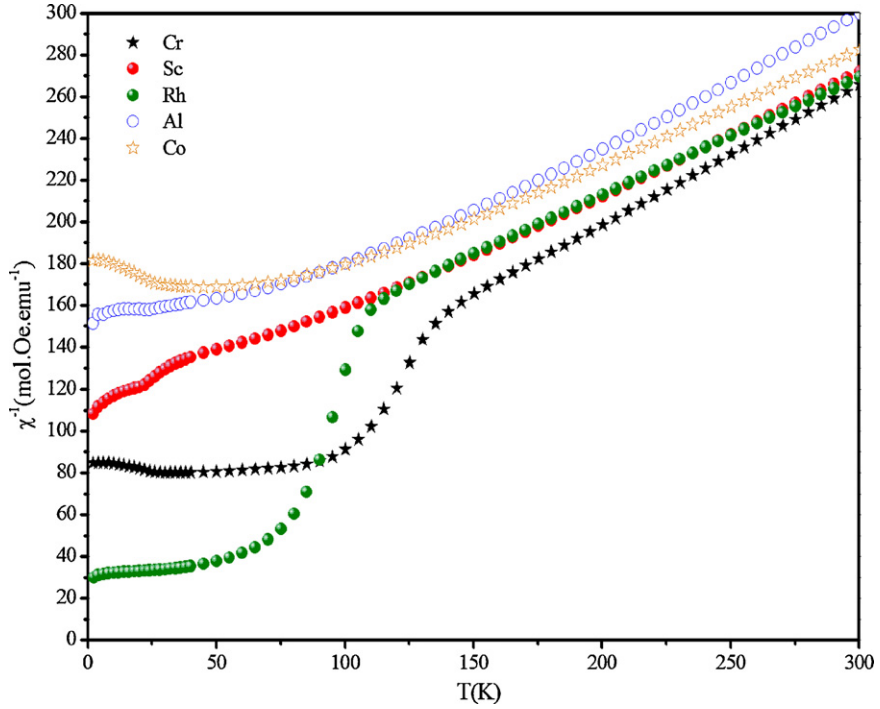

Fig. 4. Inverse susceptibility evolution of $CuCrO_2$ with the chemical impurities.

Table 2
Estimated Curie–Weiss constants for different doped samples.

	Cr	Al	Co	Rh	Sc
C	1.498	1.5958	1.835	1.7714	1.708
Θ	97.778	175.721	217.74	177.155	162.953

4. Conclusion

In this work, different $CuCr_{1-x}M_xO_2$ compositions with M: Sc, Al, Rh and Co were prepared by a standard solid-state reaction. These oxides crystallize with the delafossite structure. The lattice parameters were found to vary according to the Vegard's. We also found that the large local lattice distortion, caused by the nonmagnetic dopant with the difference in ionic radius between magnetic and nonmagnetic ions, affects significantly the shape of XRD pattern.

We have performed magnetic susceptibility measurements on nonmagnetic impurity-doped multiferroic $CuCr_{1-x}M_xO_2$. The temperature dependence of the susceptibility of all samples exhibits paramagnetic behavior at high temperature.

Magnetic studies confirm the HS state of Co^{3+} ions and reveal that the predominant interactions are antiferromagnetic and their strength change with the dopant.

Taking into account the Sc^{3+}, Co^{3+}, Rh^{3+} and Al^{3+} substitution dependence of χ, the main origin of the stabilization of the AF state is perhaps not the introduced randomness but the doped itinerant holes. The coupling between the local spins at the Cr sites and doped holes may enhance spin fluctuations at the Cr sites [13], which may break the residual magnetic degeneracy as fluctuation-induced symmetry breaking in a highly magnetic degenerate ground state manifold of some frustrated systems [26,27].

Acknowledgement

This work was financially supported by Université Joseph Fourier (UJF-Chimie), Grenoble, France.

References

[1] T. Okuda, N. Jufuku, S. Hidaka, N. Terada, Phys. Rev. B 72 (2005) 144403–144408.
[2] N. Terada, Y. Nakamura, K. Katsumata, T. Yamamoto, U. Staub, K. Kindo, M. Hagiwara, Y. Tanaka, A. Kikkawa, H. Toyama, T. Fuyuki, R. Kanmuri, T. Ishikawa, H. Kitamura, Phys. Rev. B 74 (2006) 180404R–180407.
[3] T. Kimura, J.C. Lashley, A.P. Ramirez, Phys. Rev. B 73 (2006) 180404R–180407.
[4] M. Amami, C.V. Colin, P. Strobel, A. Ben Salah, Phys. B: Condens. Matter 406 (2011) 2182–2185.
[5] N. Terada, S. Mitsuda, T. Fujii, K. Soejima, I. Doi, H.A. Katori, Y. Noda, J. Phys. Soc. Jpn. 74 (2005) 2604.
[6] A.G. Zalazinskii, V.F. Balakirev, N.M. Chebotaev, G.I. Chufarov, Russ. J. Inorg. Chem. 14 (1969) 326–328.
[7] T. Okuda, T. Onoe, Y. Beppu, N. Terada, T. Doi, S. Miyasaka, Y. Tokura, J. Magn. Magn. Mater. 310 (2007) 890–892.
[8] F.A. Benko, F.P. Koffyberg, Mater. Res. Bull. 21 (1986) 753–757.
[9] R. Nagarajan, N. Duan, M.K. Jayaraj, J. Li, K.A. Vanaja, A. Yokochi, A. Draeseke, J. Tate, A.W. Sleight, Int. J. Inorg. Mater. 3 (2001) 265–270.
[10] J. Tate, M.K. Jayaraj, A.D. Draeseke, T. Ulbrich, A.W. Sleight, K.A. Vanaja, R. Nagarajan, J.F. Wager, R.L. Hoffman, Thin Solid Films 411 (2002) 119–124.
[11] S. Mahapatra, S.A. Shivashankar, Chem. Vap. Depos. 9 (2003) 238–240.
[12] D. Li, X.D. Fang, Z.H. Deng, S. Zhou, R.H. Tao, W.W. Dong, T. Wang, Y.P. Zhao, G. Meng, X.B. Zhu, J. Phys. D: Appl. Phys. 40 (2007) 4910–4915.
[13] H. Yamaguchi, S. Ohtomo, S. Kimura, M. Hagiwara, K. Kimura, T. Kimura, T. Okuda, K. Kindo, Phys. Rev. B 81 (2010) 033104.
[14] Y. Ono, K. Satoh, T. Nozaki, T. Kajitani, Jpn. J. Appl. Phys. 46 (2007) 1071–1075.
[15] R. Rao, A. Dandekar, R.T.K. Baker, M.A. Vannice, J. Catal. 171 (1997) 406–419.
[16] J. Shu, X. Zhu, T. Yi, Electrochim. Acta 54 (2009) 2795–2799.
[17] A. Maignan, C. Martin, R. Frésard, V. Eyert, E. Guilmeau, S. Hébert, M. Poienar, D. Pelloquin, Solid State Commun. 149 (2009) 962–967.
[18] R. Nagarajan, A.D. Draeseke, A.W. Sleight, J. Tate, J. Appl. Phys. 89 (2001) 8022–8025.
[19] R.D. Shannon, D.B. Rogers, C.T. Prewitt, Inorg. Chem. 10 (1971) 713–718.
[20] T. Okuda, Y. Beppu, Y. Fujii, T. Onoe, N. Terada, S. Miyasaka, Phys. Rev. B 77 (2008) 134423–134427.
[21] J. Tate, M.K. Jayaraj, A.D. Draeseke, T. Ulbrich, A.W. Sleight, K.A. Vanaja, R. Nagarajan, J.F. Wagner, R.L. Hoffman, Thin Solid Films 411 (2002) 119–124.
[22] J. Pellicer-Poress, D. Martinez-Garcia, A. Segura, P. Rodrigez-hernandez, A. Munoz, J.C. Chervin, Phys. Rev. B 74 (2006) 184301–184308.
[23] J. Pellicer-Porres, A. Segura, E. Martinez, Phys. Rev. B 72 (2005) 064301–064306.
[24] J.E. Maslar, W.S. Hurst, T.A. Vanderah, I. Levin, J. Raman Spectrom. 32 (2001) 201–206.
[25] H. Kadoeaki, H. Kikuchi, Y. Ajiro, J. Phys.: Condens. Matter 2 (1990) 4485–4494.
[26] J. Villain, R. Bidaux, J.P. Carton, R. Conte, J. Phys. (France) 41 (1980) 1263–1267.
[27] J.E. Greedan, J. Alloy Compd. 408–412 (2006) 444–455.